DOI: 10.1002/ejic.200900156

# Nonanuclear Coordination Compounds Featuring $\{M_9L_{12}\}^{6+}$ Cores (M = $Ni^{II}$, $Co^{II}$, or $Zn^{II}$; L = 1,2,3-Benzotriazolate)

**Shyam Biswas,[a] Markus Tonigold,[a] Manfred Speldrich,[b] Paul Kögerler,[b] and Dirk Volkmer*[a]**

**Keywords:** Benzotriazole / Cluster compounds / Transition metals / N ligands / Magnetic properties

Syntheses, characterization, and magnetic properties of three nonanuclear coordination compounds with the molecular formulae $[Ni_9(bta)_{12}(NO_3)_6(MeOH)_6]\cdot 4THF$ (**1**) (btaH = 1,2,3-benzotriazole; THF = tetrahydrofuran), $[Co_9(bta)_{12}(MeOH)_{18}][(NO_3)_6]\cdot 9C_6H_6$ ($C_6H_6$ = benzene) (**2**), and $[Zn_9(Me_2bta)_{12}(CH_3COO)_6]\cdot 3DMF$ ($Me_2$btaH = 5,6-dimethyl-1,2,3-benzotriazole; DMF = *N*,*N*′-dimethylformamide) (**3**) are presented. The solid-state structures of all the compounds were determined by single-crystal X-ray structure analysis revealing the presence of structurally similar $\{M_9L_{12}\}^{6+}$ cores (M = $Ni^{II}$, $Co^{II}$, or $Zn^{II}$; L = 1,2,3-benzotriazolate) in which the metal centers are bridged by $\mu_3$-benzotriazolates. The charges of the cationic $\{M_9L_{12}\}^{6+}$ moieties in **1** and **3** are balanced by six nitrate and acetate anions coordinated to the peripheral metal atoms, respectively, whereas **2** is a cationic metal complex with six noncoordinated nitrate counterions in the crystal lattice. All the metal centers in each compound are hexacoordinate, except for the peripheral metal centers in **3** which are pentacoordinate.

The nonanuclear cores can be formally subdivided into two metallosupramolecular tetrahedra which bear five metal ions each, and share a common apex. All compounds have been prepared by using excess of ligand, which acts as an auxiliary base, serving to abstract protons from the coordinated benzotriazole ligand. Magnetic susceptibility studies (2–290 K) show net antiferromagnetic intramolecular coupling for **2**, while **1** displays both ferro- and antiferromagnetic coupling contributions. Both compounds exhibit strong ligand field effects in their magnetic properties. Phase purity of the compounds was ascertained by X-ray powder diffraction (XRPD) analysis, IR spectroscopy, and elemental analysis.



## Introduction

Realizing and understanding magnetic phenomena in quasi-zero dimensional molecular systems is key to the development of molecule-based magnetic materials that promise tailored physical properties[1] that will allow the use of this class of compounds as "smart" switches, molecular sensors, and as components in molecular spintronics. Of particular interest in this context are strategies that allow one to systematically vary and thus tune the magnetic properties of such molecular systems.[2] Given the intricate structure–property relationships that govern the intramolecular interactions between the spin centers in a magnetic molecule, synthesis of isostructural compounds comprising different spin centers is of particular importance for the development of rational approaches to predefined magnetic properties. The similarity of the coordination chemistry of $Ni^{II}$ and $Co^{II}$ suit these spin centers for the production of common structural motifs.[3] We report herein on polynuclear $M^{II}$ complexes (M = Ni, Co, Zn) featuring both bridging benzotriazolate and different terminal ligands. Benzotriazole and its derivatives (Scheme 2) are well-studied corrosion inhibitors for certain metals, particularly copper[4] and its alloys.[5] They are also important tridentate ligands in the field of polynuclear metal complexes and cluster compounds as they can bind to metal ions in a variety of different coordination modes. Focusing our summary on coordination compounds of $\mu_3$-benzotriazolates with divalent metal ions, a range of pentanuclear metal complexes of the formula $[M_5(L)_{4-x}(OH)_x(L')_6(H_2O)_{4x}]$ (where M = Cu, Ni, Zn; L′ = bta or $Me_2$bta; L = β-diketonate, $x$ = 0, 1) were described in the literature.[6,9] Moreover, a mixed-valent pentanuclear copper[7] and a nonanuclear nickel[8] benzotriazolate complex have been reported. Magnetic susceptibility studies performed on both the pentanuclear copper and the nonanuclear nickel complexes show antiferromagnetic interactions.[6–8] Most of these complexes are prepared in solution employing metal(II) β-diketonates as precursors, thus taking advantage of the proton transfer between metal(II) β-diketonates and benzotriazole ligands,

[a] Institute of Inorganic Chemistry II, Materials and Catalysis, Ulm University,
Albert-Einstein-Allee 11, 89081 Ulm, Germany
Fax: +49-(0)731-5023039
E-mail: dirk.volkmer@uni-ulm.de
[b] Institute of Inorganic Chemistry, RWTH Aachen University, 52074 Aachen, Germany

Supporting information for this article is available on the WWW under http://dx.doi.org/10.1002/ejic.200900156.

   

which subsequently leads to partial replacement of β-diketonato ligands by deprotonated benzotriazoles. Recently, we reported $T_d$-symmetrical pentanuclear metal complexes of the type $[M'Zn_4Cl_4(L_6)]$,[9] where M′ = Zn or $Co^{II}$, and L represents a 1,2,3-benzotriazolate ligand. For the synthesis of these compounds metal precursors and ligands were combined at the theoretical stoichiometric ratio in the presence of an auxiliary base such as lutidine. The formation of $T_d$-symmetrical homo- and heteronuclear complexes (Scheme 1) is facilitated by the fact that Zn ions – in the presence of chloride counter anions – prefer a tetrahedral coordination environment for steric reasons, whereas the central octahedral coordination site can be occupied selectively by a transition metal ion susceptible to ligand-field stabilization energy in such a coordination environment.

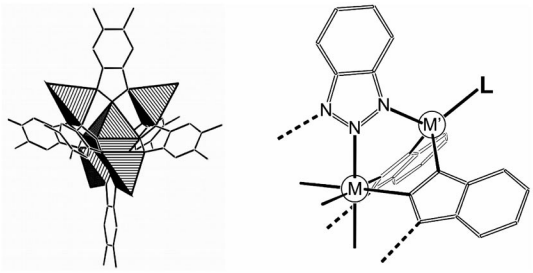


Scheme 1. Different coordination sites in the $T_d$-symmetric pentanuclear coordination compounds of type $[MM'_4Cl_4(bta)_6]$ (M = $Co^{II}$, M′ = Zn) as described in ref.[9]

However, the homonuclear Ni, Co, and Zn compounds described in the current manuscript have all been synthesized using an excess of ligand, which acts as an auxiliary base leading to deprotonation of the acidic protons of coordinated ligands. Employing this strategy, we have been able to prepare three novel compounds, namely $[Ni_9(bta)_{12}(NO_3)_6(MeOH)_6]\cdot 4THF$ (**1**), $[Co_9(bta)_{12}(MeOH)_{18}][(NO_3)_6]\cdot 9C_6H_6$ (**2**), and $[Zn_9(Me_2bta)_{12}(CH_3COO)_6]\cdot 3DMF$ (**3**), which were characterized by single-crystal X-ray structure analysis, UV/Vis spectroscopy as well as temperature-dependent magnetic susceptibility measurements. To the best of our knowledge, compound **2** and **3** are the first examples of nonanuclear $Co^{II}$ and Zn coordination compounds containing $\mu_3$-bridging benzotriazolates (Scheme 2).

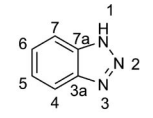


1*H*-benzo[*d*][1,2,3]triazole (btaH)

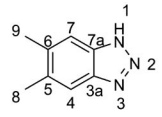


5,6-dimethyl-1*H*-benzo[*d*][1,2,3]triazole ($Me_2$btaH)

Scheme 2. Structures of 1,2,3-benzotriazole ligands used in this work.

## Results and Discussion

### Syntheses

Many polynuclear metal complexes containing benzotriazolate ligands have been prepared using metal(II) β-diketonates as precursors, thus taking advantage of the fact that the reaction between metal(II) β-diketonates and benzotriazole ligands leads to a partial replacement of β-diketonato ligands by deprotonated benzotriazoles, and, finally, to formation of large heteroleptic metal coordination compounds.[6,8,9] However, the synthesis of the nonanuclear compounds is based on a different strategy.

Compound **1** was synthesized by using an M/L ratio of 1:4, whereas in the preparation of compounds **2** and **3**, an M/L ratio of 1:8 was employed. In both synthetic procedures, a huge excess of ligand with regard to the calculated stoichiometric ratio (M/L = 1:1.33) was employed, the excess benzotriazole molecules acting as an auxiliary base in the reaction mixture, leading to deprotonation of the acidic –NH protons from coordinated benzotriazole ligands. Deprotonation is a necessary requirement for the ligand coordinating to three adjacent metal centers via its three N-donor atoms ($\mu_3$-bridging mode).

All compounds are stable in air under ambient conditions. Compounds **1** and **2** are soluble in water, methanol, and DMF. Compound **3** is insoluble in common organic solvents including chloroform, methanol, acetonitrile, DMF, and DMSO (DMSO = dimethyl sulfoxide).

### Characterization

Phase purity of all three metal complexes was confirmed by elemental analysis and by X-ray powder diffraction (XRPD). The experimental XRPD pattern is consistent with the simulated one as determined from the single-crystal X-ray diffraction data (Figure S1, Supporting Information).

The FTIR spectrum of compound **1** (Figure S2, Supporting Information) shows characteristic strong bands of the btaH ligand at 1001 and 1200 $cm^{-1}$ assigned to C–H out-of-plane bending vibrations, and vibrations involving both triazole ring breathing and C–H in-plane bending, respectively.[10] Similar values are found for compound **2** (Figure S3, Supporting Information): 1002 and 1195 $cm^{-1}$, and for compound **3** (Figure S4, Supporting Information), respectively: 998 and 1195 $cm^{-1}$. Compound **1** shows an absorption shoulder at 1479 $cm^{-1}$ which is a typical value for a nitrate anion coordinating to an octahedral $Ni^{II}$ center.[11] The absorption band for coordinated methanol molecules overlaps with the broad absorption bands of the bta ligand in the region around 2600–3700 $cm^{-1}$ for both **1** and **2**. The coordinated acetate anions in compound **3** show strong bands at 1669 and 1449 $cm^{-1}$ for the asymmetric and symmetric stretching vibrations, respectively.[12]

The UV/Vis spectra of compounds **1** and **2** in methanol solution display a common absorption band in the UV region at around 380 nm, which corresponds to the intrali-

  

gand n→π* transition.[13] In addition, both **1** and **2** exhibit well-developed bands in the range of 370–1100 nm (see parts a in Figures 1 and 2) owing to the d–d transitions of $Co^{II}$ and $Ni^{II}$ ions.[14] Compound **1**, which contains all octahedrally coordinated $Ni^{II}$ ions, shows three absorption bands at 980, 615, and 380 nm due to the spin-allowed transitions from $^3A_{2g}$ to $^3T_{2g}(F)$ ($\nu_1$), $^3T_{1g}(F)$ ($\nu_2$), and $^3T_{1g}(P)$ ($\nu_3$), respectively. The $\nu_3$ transition of **1** is probably overlapped with the intraligand n→π* transition. The values of $Dq$ (1085 $cm^{-1}$) and $B$ (775 $cm^{-1}$) which have been estimated from these transitions are typical for six-coordinate octahedral $Ni^{II}$ compounds.[14] Compound **2** shows three absorption bands at 1020, 715, and 520 nm, which can be attributed to the spin-allowed transitions from $^4T_{1g}(F)$ to $^4T_{2g}(F)$ ($\nu_1$), $^4T_{1g}(P)$ ($\nu_2$), and $^4A_{2g}$ ($\nu_3$), respectively. The calculated values of $Dq$ (1070 $cm^{-1}$) and $B$ (715 $cm^{-1}$) from these transitions is comparable to those of other six-coordinate octahedral $Co^{II}$ compounds.[14] The UV/Vis diffuse reflectance spectra (DRS) of the two compounds (see parts b in Figures 1 and 2) show similar absorption bands if compared to the solution UV/Vis spectra, which indicates that the compounds maintain their structural integrity in solution. All the spectroscopic data mentioned above provide substantial evidence for the fact that the $Ni^{II}$ and $Co^{II}$ centers retain their octahedral coordination environments in solution.

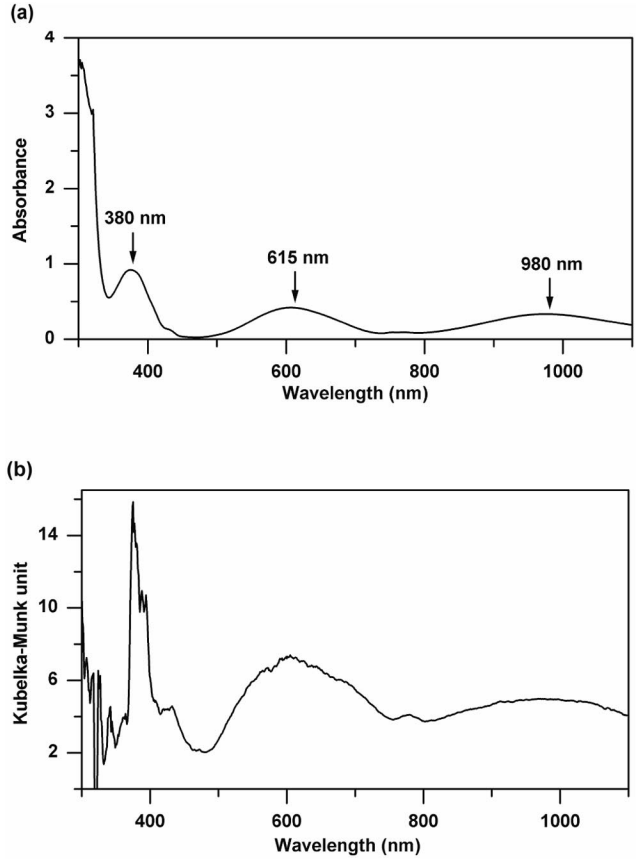


Figure 1. (a) UV/Vis spectrum of **1** in methanol solution. (b) UV/Vis diffuse reflectance spectrum of **1** (calculated via the Kubelka–Munk function).

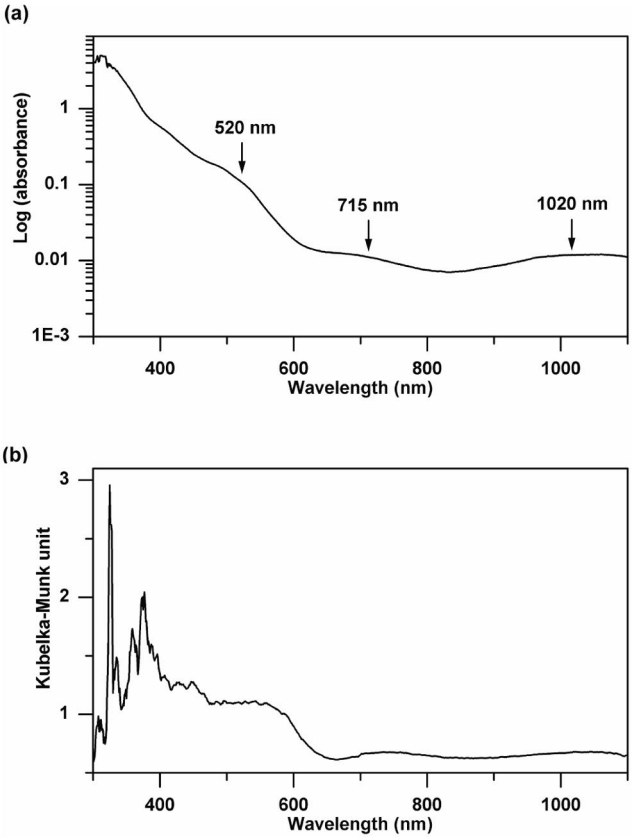


Figure 2. (a) UV/Vis spectrum of **2** in methanol solution. (b) UV/Vis diffuse reflectance spectrum of **2** (calculated via the Kubelka–Munk function).

In order to examine the thermal stability of the compounds, thermogravimetric analysis (TGA) was performed on polycrystalline samples of compounds **1**, **2**, and **3** in a nitrogen atmosphere. Three weight loss steps can be observed in the TGA curve of **1** (Figure S5, Supporting Information). The first weight loss of 18.5% in the temperature range 30–300 °C is attributed to the loss of four isolated THF and six coordinated methanol molecules (calcd. 17.2%). The second (9.3%) and third (26.4%) weight loss steps may be due to decomposition of the compound. The TGA curve of **2** (Figure S6, Supporting Information) also shows a three-step weight loss process. The first weight loss is 6.5% from 43 to 205 °C, and the second step is 13.5% from 205 to 367 °C, both assigned to the loss of 18 coordinated methanol molecules (calcd. 19.9%). The third weight loss of 30.0% is assigned to the decomposition of **2**. In the TGA curve of **3** (Figure S7, Supporting Information), no considerable weight loss is observed until 400 °C, which indicates that the compound is stable up to this temperature. After that three consecutive weight loss steps (11.7, 11.7, and 16.7%) occur in the range 400–600 °C, which may be attributed to the decomposition of the compound.

## Description of the Structures

The structures of the nonanuclear compounds can be deduced from the pentanuclear ones having $\{M_5(bta)_6\}^{4+}$

  

cores that have been described previously in the literature.[6a–6d,9] In the pentanuclear compounds, six monodentate benzotriazole ligands are coordinated to the central ion (M) (Scheme 1). The six benzotriazole ligands span a Cartesian coordinate system with the Cartesian axes running through the octahedral metal ion at the origin and the $N^2$ atoms of the coordinated ligands. The bta ligands are twisted around their coordinative bond to the central metal ion such that the nitrogen atoms are placed on the edges of an imaginary tetrahedron. At the corners of this tetrahedron are placed four additional ions M′ that are coordinated to the $N^1$ and $N^3$ donor atoms of the bta ligands. The coordination geometry of the peripheral ions (M′) is quite flexible: four-, five-, and sixfold coordination can be observed. Following this, the structures of the nonanuclear compounds described herein can be formally derived from two pentanuclear cluster cores $\{M_5(bta)_6\}^{4+}$ serving as (formal) structural building units (SBUs) of the final nonanuclear compounds. Assuming that one parent pentanuclear SBU loses a peripheral metal ion, both a tetranuclear and a pentanuclear SBU could be fused together via a central octahedrally coordinated metal ion, as depicted in Figure 3.

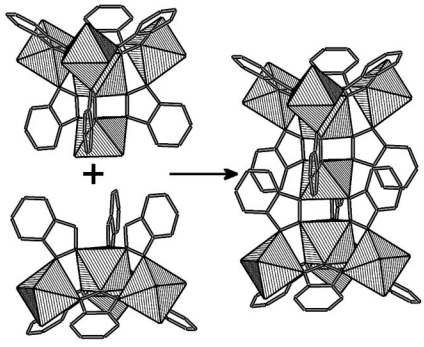

Figure 3. Schematic formation of the benzotriazolate nonanuclear coordination compounds (right) by the (hypothetical) fusion of tetranuclear and pentanuclear structural building units (left). H-atoms and coordinated molecules other than bta/$Me_2$bta are omitted for clarity.

X-ray crystallographic analysis reveals that the nonanuclear compounds **1** and **2** crystallize in the highly symmetric hexagonal space groups *R*-3 and *R*-3*c*, respectively, whereas **3** crystallizes in the triclinic space group $P\bar{1}$. The molecular structures of the nonanuclear compounds **1**–**3** are shown in Figure 4. For all compounds slight differences occur in the coordination geometries of the peripheral metal ions. In compounds **1** and **2**, peripheral metal atoms are hexacoordinate while the peripheral Zn ions in **3** are pentacoordinate. Three methanol molecules are coordinated to the peripheral $Co^{II}$ ions in **2**, and nitrate counteranions are placed at suitable positions in the crystal lattice. In contrast, the nitrate anion in **1** is coordinated directly to the peripheral $Ni^{II}$ centers together with an additional methanol molecule. In the case of **3**, each peripheral Zn atom is directly coordinated by one bidentate acetate anion, which binds in $\eta^2$-mode.

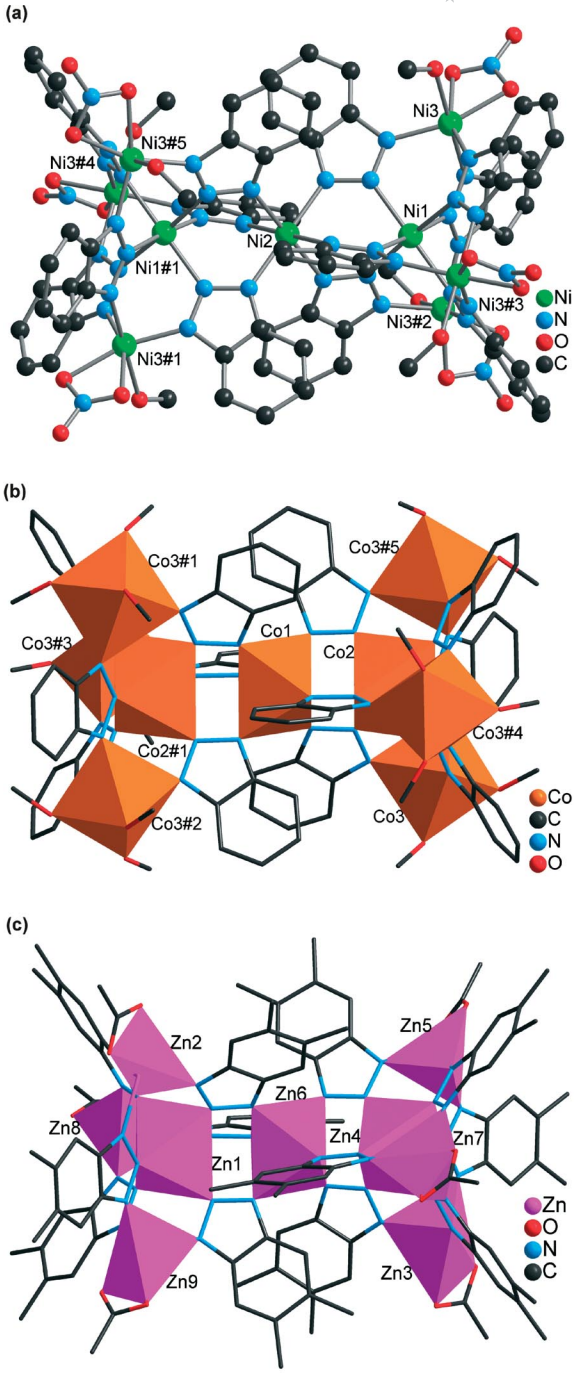


Figure 4. Ball-and-stick representation of the molecular structure of **1** (a). Wire representations of the molecular structures of **2** (b) and **3** (c) with metal atoms represented as polyhedra. For **1**, the symmetry operators used to create equivalent metal atoms are #1: $-x, -y, -z$; #2: $-x + y, -x, z$; #3: $-y, x - y, z$; #4: $y, -x + y, -z$ and #5: $x - y, x, -z$. For **2**, they are #1: $2 - x, 2 - y, -z$; #2: $y, 1 - x + y, -z$; #3: $1 + x - y, x, -z$; #4: $1 - x + y, 2 - x, z$ and #5: $2 - y, 1 + x - y, z$.

In the crystal lattices of **1** and **2**, the coordination clusters are arranged along imaginary lines parallel to the crystallographic *c* axis, as shown in Figure 5. They are more densely packed in **2** than in **1**. In compound **2**, neighboring mole-

  

cules maintain a distance of 0.35 nm to each other. In **1**, on the other hand, adjacent molecules are 0.8 nm apart from each other, leading to large voids in the structure. Because of the increased steric hindrance caused by the additional two methyl groups on the ligand in compound **3** ($Me_2$bta instead of bta), the neighboring molecules do not arrange along one line, reducing the space group symmetry of the lattice to $P\bar{1}$.

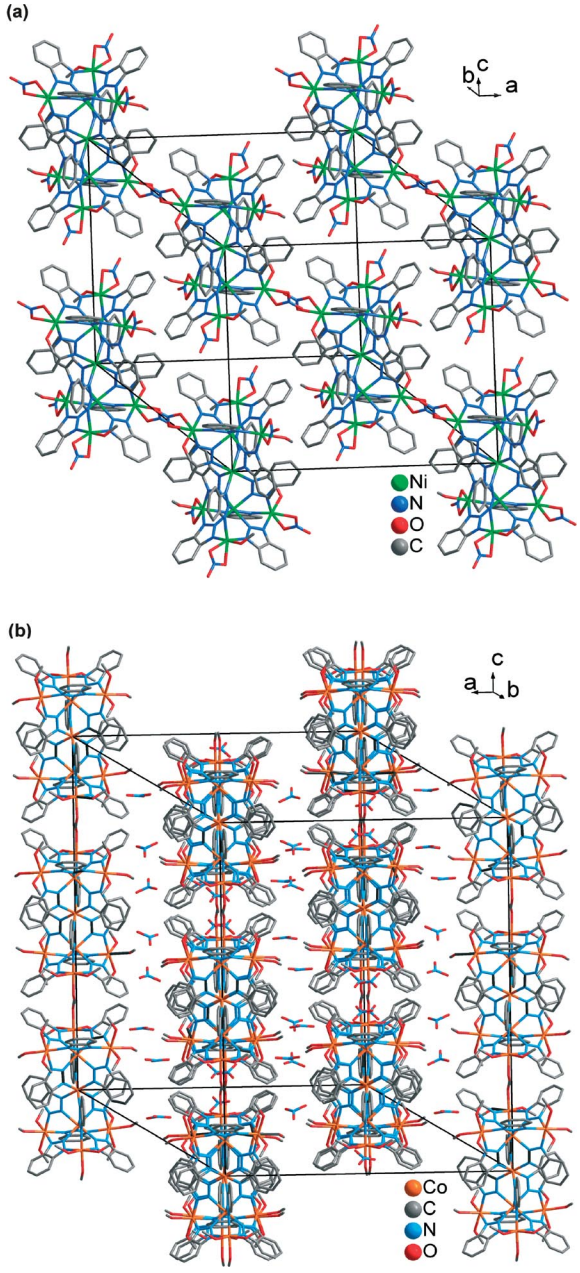


Figure 5. Crystal packing diagram of **1** (a) and **2** (b) in wire representation (all H atoms and occluded solvent molecules are omitted for clarity).

For all compounds **1**–**3**, some residual electron density was found in the unit cell, which we ascribe to vastly disordered solvent molecules, the atom positions of which could not be refined. For **3**, several restraints on intramolecular bond lengths of occluded DMF molecules had to be applied.

The observed $\eta^3$:$\mu_3$ coordination mode of deprotonated benzotriazole has been previously reported in copper,[6a–6d,7] thallium(I),[15] nickel,[6e–6f,8] zinc,[9,16] and in $M^{III}$ (M = Fe, Cr, V)[17] coordination chemistry. Compound **2** is the first example of this coordination mode for cobalt(II) complexes.

## Magnetic Properties

The magnetochemical description of the $Ni^{II}$- and $Co^{II}$-based compounds on the sole basis of low-field susceptibility data is inherently limited to a phenomenological description due to the presence of a multitude of distinct exchange pathways as well as the different local coordination environments. The interpretation of the magnetism of the $Co^{II}$-based compound **2** is complicated by the fact that the free-ion $^4F$ ground term of $Co^{II}$ is separated by the first excited $^4P$ state by more than 104 $cm^{-1}$.[18] In a weak ligand field with octahedral symmetry, the $^4F$ term splits into $^4T_1(F)$, $^4T_2$, and $^4A_2$ terms, while the $^4P$ term transforms into a $^4T_1(P)$ term (cf. discussion of UV/Vis spectra). The $^4T_1(F)$ ground term for a high-spin $Co^{II}$ center implies a significant contribution of the orbital momentum.[19] The situation for the $Ni^{II}$-based compound **1** is less complicated since the $d^8$ configuration results in an orbital singlet ground state ($A_2$).[19]

The magnetic data for compounds **1** and **2** were analyzed using a complete basis set (full d manifolds, i.e. 120 functions for $Co^{II}$ and 45 functions for $Ni^{II}$) as a function of the applied field.[20] Both aspects are necessary to yield reliable information on the magnetic dipole orientation with respect to the local symmetry elements. The simulations take into account the following single-ion effects: interelectronic repulsion ($H_{ee}$), spin-orbit coupling ($H_{SB}$), ligand-field effects ($H_{lf}$), and the applied field ($H_{mag}$). Generally, for a magnetically isolated $3d^N$ metal ion in a ligand field (lf) environment in an external magnetic field $B$ the Hamiltonian of the metal ion is represented by[21,22]

$$\hat{H} = \underbrace{\sum_{i=1}^{N}\left[-\frac{\hbar^2}{2m_e}\nabla_i^2 + V(r_i)\right]}_{\hat{H}^{(0)}} + \underbrace{\sum_{i>j}^{N}\frac{e^2}{r_{ij}}}_{\hat{H}_{ee}} + \underbrace{\sum_{i=1}^{N}\zeta(r_i)\,\kappa\;\hat{\boldsymbol{l}}_i\cdot\;\hat{\boldsymbol{s}}_i}_{\hat{H}_{so}} + \underbrace{\sum_{i=1}^{N}\sum_{k=0}^{\infty}\left\{B_0^k C_0^k(i) + \sum_{q=2}^{k}\left[B_q^k\left(C_{-q}^k(i) + (-1)^q C_q^k(i)\right)\right]\right\}}_{\hat{H}_{LF}} + \underbrace{\sum_{i=1}^{N}\mu_B(\kappa\,\hat{\boldsymbol{l}}_i + 2\,\hat{\boldsymbol{s}}_i)\cdot\;\boldsymbol{B}}_{\hat{H}_{mag}}$$

Figure 6 displays the results of the magnetic susceptibility measurement in the temperature range 2–290 K using $\mu_{eff}$ vs. $T$ plots [SI units: $\mu_{eff} = 797.74(\chi T)^{1/2}$]. The effective magnetic moment of **2** at 290 K is 5.27 $\mu_B$ per $Co^{II}$

  

ion, which is larger than the spin-only value of 3.87 $\mu_B$ as a result of spin and first-order orbital contributions. The monotonous decrease of $\mu_{eff}$ towards lower temperatures can thus be attributed to both single-ion effects and antiferromagnetic intramolecular exchange coupling. To quantify these effects, we analyzed the magnetic data considering ligand-field effect, spin-orbit coupling, and external magnetic field. Note that as stated above the presence of at least four different exchange pathways, all mediated by the benzotriazolate ligands, in both **1** and **2** precludes the unambiguous determination of their associated exchange energies ($J_{1–4}$) based solely on $\chi(B,T)$ data. In such cases, over-parameterization leads to isospectrality issues, i.e. several sets of $J_{1–4}$ reproduce the same thermodynamical susceptibility data. We are currently planning additional low-temperature, high-field magnetization and neutron scattering measurements in order to develop a Heisenberg-type exchange model that identifies all relevant exchange energies. Here, however, we have to limit the interpretation of the exchange interactions to the phenomenological molecular field approximation

$$\chi_m^{-1} = \chi_m^{-1}(\varsigma, B_q^{\kappa}) - \lambda_{MF}$$

where $\chi_m$ is the single-center susceptibility and $\lambda$ is the molecular field parameter. Positive and negative $\lambda$ indicates dominant ferromagnetic and antiferromagnetic interactions, respectively. Note that this effectively reduces the number of exchange parameters from four to one. The parameters $\lambda_{MF}$ and $B_q^k$ were determined by a least-squares fit. For **2** the best fit for calculated and experimental values was found for $\lambda_{MF} = -0.463 \times 10^6$ mol m$^{-3}$, $B_0^2 = 3096$ cm$^{-1}$, $B_0^4 = 10405$ cm$^{-1}$, $B_4^4 = 5462$ cm$^{-1}$ ($SQ$ = 0.5%). Note that the negative molecular field parameter $\lambda_{MF}$ is essential for a good fit. The ligand field splitting based on the magnetochemical analysis of **2**, yielding $Dq$ = 1167 cm$^{-1}$, corresponds well to the parameter established from UV/Vis spectra.

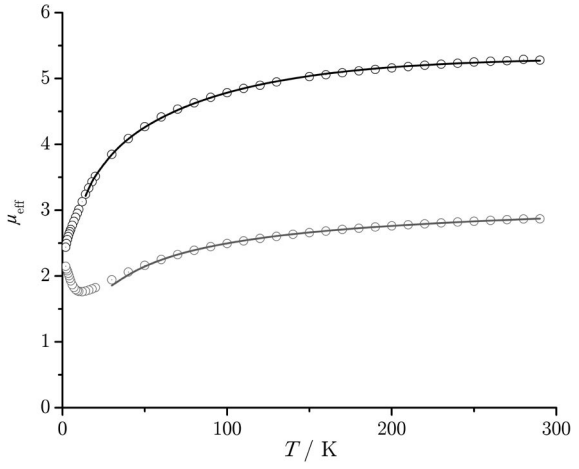


Figure 6. Temperature dependence of $\mu_{eff}$ for compounds **1** (grey) and **2** (black) at 0.1 Tesla. Open circles: experimental data, graphs: best fits to the employed phenomenological models (see text).

The effective magnetic moment of **1** decreases from 2.83 $\mu_B$ per $Ni^{II}$ ion (290 K) to a minimum of 1.76 $\mu_B$ at 12 K, indicating net antiferromagnetic interactions in this temperature interval. However, ferromagnetic coupling becomes dominant below 12 K and $\mu_{eff}$ increases with decreasing temperature, which possibly stems from coupling between the tetranuclear $Ni_4$ fragments in **1**. Similar differences in coupling have also been observed in other isostructural $Ni^{II}$ and $Co^{II}$ complexes.[23] For the interval 30–290 K, the best fit for calculated and experimental values $\chi_m$ was found for $\lambda_{MF} = -0.463 \times 10^6$ mol m$^{-3}$, $B_0^2 = 8286$ cm$^{-1}$, $B_0^4 = 25185$ cm$^{-1}$, $B_4^4 = 15552$ cm$^{-1}$ ($SQ$ = 0.4%).

## Conclusions

The work herein illustrates that the use of benzotriazolate-type ligands represents a successful synthetic strategy for the preparation of polynuclear transition-metal coordination compounds. We have synthesized three nonanuclear $Ni^{II}$, $Co^{II}$, and Zn compounds (**1**, **2**, and **3**) containing $\mu_3$-benzotriazolates and described their structures and magnetic properties. Magnetochemical analysis shows net antiferromagnetic intramolecular coupling in $Co^{II}$-based compound **2**, whereas both ferro- and antiferromagnetic coupling is observed in $Ni^{II}$-based compound **1**. We also demonstrated the presence of a $\eta^3$:$\mu_3$ coordination mode of benzotriazolates in $Co^{II}$ coordination chemistry. The synthetic strategy used to prepare the present compounds shows that the preparation of polynuclear coordination compounds of benzotriazoles with divalent metal ions is not only restricted to the use of metal(II) β-diketonates as starting materials, nonanuclear metal complexes can likewise easily be prepared from metal(II) nitrates as well as acetates, provided that excess ligand is present in the reaction mixture as an auxiliary base. In a previous report,[9] we used metal(II) halides to prepare pentanuclear metal complexes of the type $M'Zn_4Cl_4(L_6)$, in spite of using metal(II) β-diketonates.

## Experimental Section

**Materials and General Methods:** All starting materials were of reagent grade and used as received from the commercial supplier. Fourier transform infrared spectra were recorded from KBr pellets in the range 4000–400 cm$^{-1}$ with a Bruker IFS FT-IR spectrometer. The following indications were used to characterize absorption bands: very strong (vs), strong (s), medium (m), weak (w), shoulder (sh), and broad (br). UV/Vis diffuse reflectance spectra (DRS) were recorded with an Analytik Jena Specord 50 UV/Vis spectrometer in the range of 300–1100 nm and converted into normal absorption spectra with the Kubelka–Munk function.[24] The lamps change at 320 nm and the mirrors change at 370, 400, 700, and 900 nm. For compound **2**, the sample was diluted with $BaSO_4$ (sample/$BaSO_4$ = 1:3) prior to measurement. UV/Vis spectra in solution were measured using the same UV/Vis spectrometer. Elemental analyses (C, H, N) were carried out with a Perkin–Elmer 2400 Elemental Analyzer. Thermogravimetric analysis (TGA) was performed with a TGA/SDTA851 Mettler Toledo analyzer in a temperature range of

  

25–800 °C in flowing nitrogen at a heating rate of 10 °C min$^{-1}$. X-ray powder diffraction (XRPD) patterns were measured with a Philips X′Pert PRO powder diffractometer operated at 40 kV, 40 mA for a Cu target ($\lambda$ = 1.5406 Å) with a scan speed of 30 s step$^{-1}$ and a step size of 0.008°. The simulated powder patterns were calculated using single-crystal X-ray diffraction data. Magnetic susceptibility data were determined by SQUID magnetometry (MPMS-XL5, Quantum Design) in the temperature range $T$ = 2.0 to 290 K and at an applied field of $B_0$ = 0.1 T. The data were corrected for the sample holder (PTFE tubes) and calculated diamagnetic contributions [$\chi_{dia}$(**1**) = $-2.75 \times 10^{-8}$ m$^3$ mol$^{-1}$, $\chi_{dia}$(**2**) = $-1.75 \times 10^{-8}$ m$^3$ mol$^{-1}$].

***Safety Note!*** *Benzotriazoles and benzotriazolate complexes are potentially explosive, and caution should be exercised when dealing with such derivatives. However, the small quantities used in this study were not found to present a hazard.*

**Syntheses**

**Synthesis of [Ni$_9$(bta)$_{12}$(NO$_3$)$_6$(MeOH)$_6$]·4THF (1):** To a solution of btaH (1.698 g, 14.25 mmol) in acetonitrile (150 mL), Ni(NO$_3$)$_2$·6H$_2$O (1.036 g, 3.56 mmol) was added as a solid. The mixture was stirred at room temperature for 30 min and left undisturbed at room temperature for 2 days. The resulting purple precipitate (0.56 g) was collected by filtration and dried in vacuo. Blue rhombohedral crystals of **1** were obtained within a week by layering a methanol solution (1 mL) of this precipitate (45 mg) over THF (1 mL) in an NMR tube. $C_{94}H_{104}N_{42}Ni_9O_{28}$ (2798.33): calcd. C 40.34, H 3.74, N 21.02; found C 40.30, H 3.82, N 21.16. IR (KBr): $\tilde{\nu}$ = 3212 (br), 3083 (w), 2970 (s), 2874 (s), 2494 (br), 2318 (br), 1947 (w), 1614 (w), 1577 (m), 1500 (vs), 1479 (sh), 1267 (vs), 1200 (s), 1181 (sh), 1153 (w), 1024 (s), 1001 (sh), 874 (s), 808 (m), 785 (s), 745 (vs), 692 (m), 640 (m), 556 (m), 431 (w) cm$^{-1}$.

**Synthesis of [Co$_9$(bta)$_{12}$(MeOH)$_{18}$][(NO$_3$)$_6$]·9C$_6$H$_6$ (2):** A solution of btaH (3.331 g, 27.96 mmol) in ethanol (100 mL) was combined with a solution of Co(NO$_3$)$_2$·6H$_2$O (1.017 g, 3.49 mmol) in the same solvent (100 mL). The mixture was refluxed for 1 h and cooled to room temperature. The resulting precipitate (0.73 g) was collected by filtration and dried in vacuo. Reddish orange rhombohedral crystals of **2** suitable for single-crystal X-ray diffraction were grown within 3 days by layering a methanol solution (1 mL) of this precipitate (60 mg) over benzene (1 mL) in a NMR tube. The crystals were covered with polybutene oil after being removed from the mother liquor for single-crystal X-ray diffraction studies. Samples for analytical studies were dried under vacuum, thus removing all occluded benzene molecules. $C_{90}H_{120}Co_9N_{42}O_{36}$ (2896.57): calcd. C 37.31, H 4.17, N 20.30; found C 37.74, H 3.92, N 20.85. IR (KBr ): $\tilde{\nu}$ = 3408 (br), 3080 (br), 2498 (br), 2345 (br), 1623 (m), 1579 (m), 1487 (vs), 1449 (sh), 1270 (vs), 1195 (s), 1002 (s), 925 (w), 809 (w), 785 (s), 746 (vs), 687 (m), 641 (m), 558 (m), 438 (w) cm$^{-1}$.

**Synthesis of [Zn$_9$(Me$_2$bta)$_{12}$(CH$_3$COO)$_6$]·3DMF (3):** A solution of Zn(CH$_3$COO)$_2$·2H$_2$O (0.102 g, 0.46 mmol) in DMF (10 mL) was combined with a solution of Me$_2$btaH (0.614 g, 3.72 mmol) in the same solvent (10 mL). The mixture was stirred at room temperature for 30 min and left undisturbed at room temperature. Slow evaporation of the solvent within 3 days resulted in colorless, block-shaped crystals of **3**. They were filtered off and dried in vacuo, thus removing all occluded DMF molecules. The yield was 0.073 g (0.025 mmol, 49%). $C_{108}H_{114}N_{36}O_{12}Zn_9$ (2696.80): calcd. C 48.09, H 4.26, N 18.69; found C 47.86, H 4.22, N 18.77. IR (KBr ): $\tilde{\nu}$ = 3425 (br), 3065 (m), 2966 (m), 2927 (m), 2921 (m), 2855 (m), 2365 (br), 1679 (m), 1569 (vs), 1471 (w), 1457 (s), 1427 (sh), 1374 (s), 1331 (w), 1287 (m), 1256 (w), 1195 (vs), 1165 (s), 1082 (w), 1050 (w), 1012 (sh), 998 (s), 931 (w), 849 (vs), 825 (sh), 721 (w), 689 (s), 617 (m), 570 (w), 494 (s), 463 (m), 439 (sh) cm$^{-1}$.

**X-ray Crystallography:** Single-crystal X-ray diffraction intensities were collected with a STOE IPDS diffractometer employing monochromated Mo-$K_\alpha$ radiation ($\lambda$ = 0.71073 Å). Initial structures were solved by direct methods and refined by full-matrix least-squares

Table 1. Single-crystal data and refinement summary for compounds **1**–**3**.

| Compound | **1** | **2** | **3** |
|---|---|---|---|
| Formula | $C_{94}H_{104}N_{42}Ni_9O_{28}$ | $C_{144}H_{174}Co_9N_{42}O_{36}$ | $C_{117}H_{135}N_{39}O_{15}Zn_9$ |
| Formula mass | 2798.33 | 3599.58 | 2916.08 |
| $T$ [K] | 193(2) | 193(2) | 293(2) |
| $\lambda$ [Å] | 0.71073 | 0.71073 | 0.71073 |
| Crystal dimensions [mm$^3$] | $0.38 \times 0.54 \times 0.54$ | $0.38 \times 0.58 \times 0.62$ | $0.31 \times 0.31 \times 0.38$ |
| Crystal system | hexagonal | hexagonal | triclinic |
| Space group | $R\bar{3}$ | $R\bar{3}c$ | $P\bar{1}$ |
| $a$ [Å] | 22.553(3) | 27.398(4) | 14.4593(3) |
| $b$ [Å] | 22.553(3) | 27.398(4) | 18.509(4) |
| $c$ [Å] | 22.578(5) | 37.107(7) | 28.740(6) |
| $\alpha$ [°] | | | 97.34(3) |
| $\beta$ [°] | | | 97.54(3) |
| $\gamma$ [°] | | | 112.90(3) |
| $V$ [Å$^3$] | 9946(3) | 24122(7) | 6888(2) |
| $Z$ | 3 | 6 | 2 |
| $D_c$ [g cm$^{-3}$] | 1.257 | 1.487 | 1.406 |
| $M$ [mm$^{-1}$] | 1.317 | 0.991 | 1.609 |
| $F$(000) | 3834 | 11178 | 3000 |
| $\theta$ Range [°] | 2.08–25.87 | 2.04–25.90 | 2.07–26.02 |
| Measured reflections | 26018 | 61510 | 54595 |
| Independent reflections | 4266 | 5209 | 25147 |
| Data/restraints/parameters | 4266/0/231 | 5209/0/349 | 25147/52/1571 |
| $R_1$ [$I > 2\sigma(I)$] [a] | 0.0988 | 0.0488 | 0.0595 |
| $wR_2$ (all data) [b] | 0.3176 | 0.1372 | 0.1695 |
| Goodness-of-fit on $F^2$ | 1.194 | 1.045 | 0.871 |
| $\Delta\rho_{max,\ min}$ [e Å$^{-3}$] | 2.36/–0.77 | 1.28/–1.10 | 1.58/–0.76 |

[a] $R_1 = \Sigma||F_o| - |F_c||/\Sigma|F_o|$. [b] $wR_2 = \{\Sigma[w(F_o^2 - F_c^2)^2]/\Sigma[w(F_o^2)^2]\}^{1/2}$.

  

techniques based on $F^2$ using the SHELXL-97[25] program. Details of data collection and refinement of the compounds are summarized in Table 1.

CCDC-730718 (for **1**), -730719 (for **2**), and -730720 (for **3**) contain the supplementary crystallographic data for this paper. These data can be obtained free of charge from The Cambridge Crystallographic Data Centre via www.ccdc.cam.ac.uk/data_request/cif.

**Supporting Information** (see also the footnote on the first page of this article): XRPD patterns, IR spectra, TGA curve, optical micrographs.

## Acknowledgments

The authors are grateful for financial support from the Deutsche Forschungsgemeinschaft (DFG) (Priority Program 1362, "Porous Metal-Organic Frameworks", VO 829/5-1). M. T. is grateful to the Landesgraduiertenförderung Baden-Württemberg for financial support.

[1] J. S. Miller, A. J. Epstein, *Angew. Chem. Int. Ed. Engl.* **1994**, *33*, 385–415.
[2] P. Rey, D. Luneau, A. Cogne in *Magnetic Molecular Materials* (Eds.: D. Gatteschi, O. Kahn, J. S. Miller, F. Palacio), Kluwer, Dordrecht, The Netherlands, **1991**.
[3] G. J. T. Cooper, G. N. Newton, P. Kögerler, D.-L. Long, L. Engelhardt, M. Luban, L. Cronin, *Angew. Chem. Int. Ed.* **2007**, *46*, 1340–1344.
[4] I. Dugdale, J. B. Cotton, *Corros. Sci.* **1963**, *3*, 69–74.
[5] D. Chadwick, T. Hashemi, *Corros. Sci.* **1978**, *18*, 39–51.
[6] a) M. Murrie, D. Collison, C. D. Garner, M. Helliwell, P. A. Tasker, S. S. Turner, *Polyhedron* **1998**, *17*, 3031–3043; b) J. H. Marshall, *Inorg. Chem.* **1978**, *17*, 3711–3713; c) J. Handley, D. Collison, C. D. Garner, M. Helliwell, R. Docherty, J. R. Lawson, P. A. Tasker, *Angew. Chem. Int. Ed. Engl.* **1993**, *32*, 1036–1038; d) W. Jinling, Y. Ming, Y. Yun, Z. Shuming, M. Fangming, *Chin. Sci. Bull.* **2002**, *47*, 890–893; e) E. G. Bakalbassis, E. Diamontopoulou, S. P. Perlepes, C. P. Raptopoulou, V. Tangoulis, A. Terzis, T. F. Zafiropoulos, *J. Chem. Soc., Chem. Commun.* **1995**, 1347–1348; f) V. Tangoulis, C. P. Raptopoulou, A. Terzis, E. G. Bakalbassis, E. Diamontopoulou, S. P. Perlepes, *Inorg. Chem.* **1998**, *37*, 3142–3153.
[7] a) V. L. Himes, A. D. Mighell, A. R. Siedle, *J. Am. Chem. Soc.* **1981**, *103*, 211–212; b) G. F. Kokoszka, J. Baranowski, C. Goldstein, J. Orsini, A. D. Mighell, V. L. Himes, A. R. Siedle, *J. Am. Chem. Soc.* **1983**, *105*, 5627–5633.
[8] V. Tangoulis, C. P. Raptopoulou, A. Terzis, E. G. Bakalbassis, E. Diamontopoulou, S. P. Perlepes, *Mol. Cryst. Liq. Cryst.* **1999**, *335*, 463–472.
[9] S. Biswas, M. Tonigold, D. Volkmer, *Z. Anorg. Allg. Chem.* **2008**, *634*, 2532–2538.
[10] J. Rubim, I. G. R. Gutz, O. Sala, W. J. Orville-Thomas, *J. Mol. Struct.* **1983**, *100*, 571–583.
[11] E. Diamantopoulou, T. F. Zafiropoulos, S. P. Perlepes, *Polyhedron* **1994**, *13*, 1593–1608.
[12] G. V. Seguel, B. L. Rivas, C. Novas, *J. Chil. Chem. Soc.* **2005**, *50*, 401–406.
[13] A. Gilbert, J. Baggott, *Essentials of Molecular Photochemistry*, CRC Press, Boca Raton, FL, **1991**, p. 87–89.
[14] a) A. B. P. Lever, *Inorganic Electronic Spectroscopy*, Elsevier Publishing Company, Amsterdam, **1968**, chapter 9, p. 317–349; b) The *Dq* and *B* values were estimated by using the transition energy ratio diagrams on p. 393–400 of the same book as in ref.[14a].
[15] J. Reedijk, G. Roelofsen, A. R. Siedle, A. L. Spek, *Inorg. Chem.* **1979**, *18*, 1947–1951.
[16] Y.-Y. Qin, J. Zhang, Z.-J. Li, L. Zhang, X.-Y. Cao, Y.-G. Yao, *Chem. Commun.* **2008**, 2532–2534.
[17] a) D. Collison, E. J. L. McInnes, E. K. Brechin, *Eur. J. Inorg. Chem.* **2006**, 2725–2733; b) J. Tabernor, L. F. Jones, S. L. Heath, C. Muryn, G. Aromí, J. Ribas, E. K. Brechin, D. Collison, *Dalton Trans.* **2004**, 975–976; c) R. H. Laye, Q. Wei, P. V. Mason, M. Shanmugam, S. J. Teat, E. K. Brechin, D. Collison, E. J. L. McInnes, *J. Am. Chem. Soc.* **2006**, *128*, 9020–9021; d) L. F. Jones, E. K. Brechin, D. Collison, A. Harrison, S. J. Teat, W. Wernsdorfer, *Chem. Commun.* **2002**, 2974–2975; e) L. F. Jones, G. Rajaraman, J. Brockman, M. Murugesu, J. Raftery, S. J. Teat, W. Wernsdorfer, G. Christou, E. K. Brechin, D. Collison, *Chem. Eur. J.* **2004**, *10*, 5180–5194; f) L. F. Jones, E. K. Brechin, D. Collison, J. Raftery, S. J. Teat, *Inorg. Chem.* **2003**, *42*, 6971–6973; g) L. F. Jones, J. Raftery, S. J. Teat, D. Collison, E. K. Brechin, *Polyhedron* **2005**, *24*, 2443–2449; h) R. Shaw, R. H. Laye, L. F. Jones, D. M. Low, C. Talbot-Eeckelaers, Q. Wei, C. J. Milios, S. Teat, M. Helliwell, J. Raftery, M. Evangelisti, M. Affronte, D. Collison, E. K. Brechin, E. J. L. McInnes, *Inorg. Chem.* **2007**, *46*, 4968–4978; i) D. M. Low, L. F. Jones, A. Bell, E. K. Brechin, T. Mallah, E. Rivière, S. J. Teat, E. J. L. McInnes, *Angew. Chem. Int. Ed.* **2003**, *42*, 3781–3784.
[18] a) B. N. Figgs, M. A. Hitchman, *Ligand-Field Theory and its Applications*, Wiley-VCH, New York, **2000**; b) C. J. Ballhausen, *Introduction to Ligand Field Theory*, McGraw-Hill, New York, **1962**.
[19] O. Kahn, *Molecular Magnetism*, VCH Publishers, New York, **1993**.
[20] H. Schilder, H. Lueken, *J. Magn. Magn. Mater.* **2004**, *281*, 17–26.
[21] B. G. Wybourne, *Spectroscopic Properties of Rare Earths*, Wiley, New York, London, Sydney, **1965**.
[22] C. Görller-Walrand, K. Binnemans, in: *Handbook on the Physics and Chemistry of Rare Earths* (Eds.: K. A. Gschneidner Jr., L. Eyring), Elsevier, Amsterdam, **1996**, vol. 23, chapter 155, p. 121.
[23] G. J. T. Cooper, G. N. Newton, D.-L. Long, P. Kögerler, M. H. Rosnes, M. Keller, L. Cronin, *Inorg. Chem.* **2009**, *48*, 1097–1104.
[24] W. W. Wendlandt, H. G. Hecht, *Reflectance Spectroscopy*, Interscience Publishers/John Wiley & Sons, New York, **1966**.
[25] G. M. Sheldrick, *SHELXL-97*, Program for X-ray Crystal Structure Refinement, University of Göttingen, Göttingen, Germany, **1997**.

Received: February 16, 2009
Published Online: June 16, 2009

  